Vision Res. Vol. 31, No. 9, pp. 1529–1540, 1991
Printed in Great Britain.

0042-6989/91 $3.00 + 0.00

ROLE OF THE EXTENSIVE AREA OUTSIDE THE X-CELL RECEPTIVE FIELD IN BRIGHTNESS INFORMATION TRANSMISSION

CHAO-YI LI,[1]* XING PEI,[1] YI-XIONG ZHOW[1] and HANS-CHRISTOPH VON MITZLAFF[2]

[1]Department of Sensory Information Processing, Shanghai Institute of Physiology, Chinese Academy of Sciences, 320 Yue-Yang Road, Shanghai, People's Republic of China and [2]Department of Neurobiology, Max-Planck-Institute for Biophysical Chemistry, 3400 Göttingen, Germany

(Received 8 December 1989; in revised form 6 September 1990)

Abstract—Stimulus area–response functions of retinal ganglion cells show an extensive disinhibitory region (DIR) outside the classical receptive field (RF). The DIR has a wide summation area but low sensitivity. Spatial responses of the retinal ganglion cells have been simulated in a model which takes into account also the properties of the DIR. By scanning the RF and its DIR with a visual image and reconstructing the transferred image for single cells, it is shown that these properties of the DIR are beneficial in the transmission of area brightness and image grey scales.

Cat Receptive field Disinhibition Brightness Contrast Visual image Periphery effect

INTRODUCTION

It has long been known that retinal ganglion cells and cells of the lateral geniculate body, have a receptive field (RF) consisting of two regions, an approximately circular centre and an annular surround, whose influence on cell activity are always antagonistic (Kuffler, 1953). As a consequence, diffuse illumination covering both centre and surround may excite the cells, if at all, only weakly. However, the cell may respond strongly when the illumination is non-uniform and when the contrast border is near its receptive field centre. For example, an ON-centre cell is maximally excited when there is a contrast border with the bright side covering the RF centre and the dark component covering part of the RF surround, and maximally inhibited in the contrary situation (Baumgartner, Brown & Schulz, 1965; Rodieck & Stone, 1965; Li, Chang, Chen, Hsu & Wang, 1979). Cells at some distance from the contrast border will be less affected. The border enhancement may become even stronger when the centre remains close to the corner of a bright contour (Li et al., 1979). These observations have led to the suggestion that retinal cells signal changes of luminance in time and space rather than code the absolute brightness of each local area of an image.

While the antagonistic centre/surround organization improves the representation of local contrast (border), it reduces sensitivity to global brightness over an extended area (area contrast). It is not clear how the visual system can transfer the various gradient of luminance of an extended area and yet represent the mean luminance in visual environment, a fundamental requirement for perception and pupil control. The luminance gradients of an area are, for example, essential for producing perception of three-dimensional visual scenes (Ramachandran, 1988). Painters have long exploited varying gradations of brightness to induce illusions in lighting, shading, shape, curvature and perspective of objects. A compensatory mechanism may, therefore, be necessary for the visual system to offset the reduction of neuronal sensitivity to respond to area contrast, and this process should of necessity not counteract the border enhancement introduced by the centre/surround interactions.

By analysing the length–response functions of lateral geniculate neurons in the cat, we have demonstrated an extensive disinhibitory region (DIR) outside the classical inhibitory surround of their receptive field (RF) (Li & He, 1987). The spatial extent is much larger than that revealed by light or dark spots (Ikeda & Wright,

*To whom all correspondence and reprint requests should be addressed.

1972a, b) and by concentrically presented annuli (Hammond, 1972, 1973) and is comparable to that of the "periphery effect" (McIlwain, 1964; Cleland, Levick & Sanderson, 1973; Fischer & Krüger, 1974), though as was described (Li & He, 1987) and will be apparent from this report, properties of the DIR make it distinct from the "periphery effect" phenomenon and may contribute to the transmission of area brightness and image grey scales. The extensive disinhibitory region was also revealed in retinal gangion cells in cat, results are reported in detail in a separate paper (Li, Zhow & Pei, 1991).

In this study, we attempted to make a quantitative estimate of the contribution of the outer region of the receptive field to spatial responses of cells by a mathematic model which takes into account also the disinhibitory mechanism. Attempts were also made to demonstrate, in single cells and in the model, by using a test image of a real object (a table-tennis ball) how the disinhibitory region may preserve information about luminance gradient. For convenience of description, representative stimulus area–response functions of retinal ganglion cells are briefly mentioned in the first section.

METHODS

We made recordings from single fibres of the optic tract and cells of the lateral geniculate nucleus of anaesthetized cats. Adult cats were initially anaesthetized with ketanest ($30\ mg\ kg^{-1}$) for surgical preparation. Anaesthesia was maintained during recordings with continuous intravenous infusion of urethan ($20\ mg\ kg^{-1}\ hr^{-1}$) in 5% lactated Ringer's solution, and paralysis was maintained with gallamine triethiodide ($10\ mg\ kg^{-1}\ hr^{-1}$) plus D-tubocurarine chloride ($0.25\ mg\ kg^{-1}\ hr^{-1}$). All wound edges and pressure points were treated with 1% lidocain. Heart rate and EEG were monitored. The end-tidal CO_2 was kept close to 4% and rectal temperature was maintained at 37.5°C. The nictitating membranes were retracted and pupils dilated with topical application of 5% neosynephrine and 1% atropine sulphate. Special care was taken to maintain good optics: the eyes were covered with contact lenses of radii appropriate for the animals' corneae and corrected for focusing on the stimulating screen in front of the eyes. Artificial pupils of 3 mm diameter were used. Recordings were made extracellularly with fine-tipped tungsten-in-glass microelectrodes and were limited to fibres which had a typical concentric RF, lying within 20 deg of the area centralis. Cell discharges, after being amplified and standardized in amplitude, were fed into a computer for data processing. The computer also served to control the presentation of different stimuli generated on the CRT screen (Tektronix 608 monitor) of an image synthesizer (Innisfree). A transparent tangent screen, placed at 57 cm from the cat's eyes, was used for conventional back projection of retinal landmarks—area centralis and blind spot—and plotting of receptive field positions (Bishop, Kozak, Levick & Vakkur, 1962). The screen was then removed for presentation of stimuli, and the CRT was centered on the cells' RF.

Visual stimuli were light bars of different lengths, or light squares of different dimension flashed with a 0.6–2 sec ON/OFF period. The intensity of the light stimulus was varied with various neutral density filters placed in front of the eye. The non-attenuated luminance was $30\ cd/m^2$. The profile of the RFs was determined by flashing horizontal and vertical bright bars (1.6 or 3.4 deg length and 0.6 deg width, 2.5 or 5 Hz) at different positions on the CRT monitor, with a 0.15–0.3 deg spacing, at intervals across the RF along the axis orthogonal to the orientation of the stimulus line, and on-line analysis of response amplitude at each position of the stimulus. For each unit recorded, the location of the receptive field centre and the spatial organization of the RF were determined on the screen of the CRT monitor. Cells were classified into *X*- and *Y*-categories according to the following response properties (Enroth-Cugell & Robson, 1966; Cleland, Dubin & Levick, 1971; Hamasaki & Sutija, 1979): *X*-cells exhibit a "null position" where contrast reversal stimulus evokes no excitation and show sustained responses to a standing contrast; *Y*-cells, by contrast, show an absence of a "null position" and transient responses. Since the aim of this work is to study how brightness, specifically area brightness, is transferred in the afferent visual pathway and only *X*-cells are responsive vigorously to standing contrast, we restrict the present studies to *X*-cells.

RESULTS

Extensive disinhibitory region outside the classical receptive field surround

Stimulus length– and/or area–response functions have been tested for lateral geniculate cells

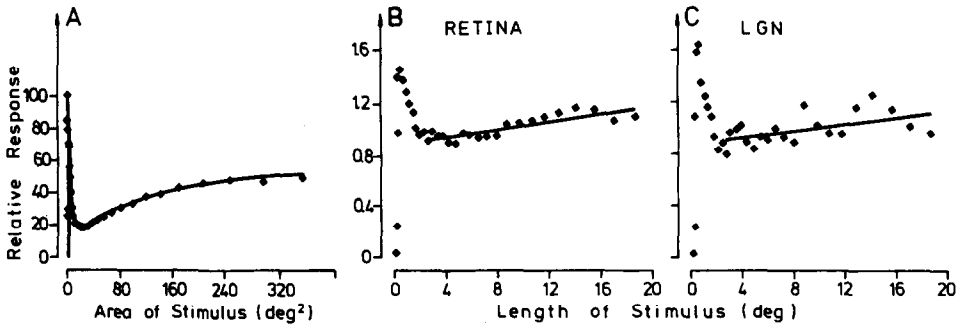

Fig. 1.(A) Area–response function of an ON-centre *X*-optic tract fibre. Stimuli were flashed bright squares of different dimensions, at 5 Hz, luminance 30 cd/m². Background illumination, 0.2 cd/m². The dots show the mean discharge rate for 5 flashes with each stimulus dimension (100% = 104 spikes/sec), and the curve, a fitting of the data based on the algebraic sum of the three Gaussian functions (see equations 1 and 2 and Table 1) representing, respectively, the spatial extent and sensitivity profile of the excitatory centre, the inhibitory surround, and disinhibitory outer-surround mechanisms of the RF. (B, C) A comparison of the length–response curves of an LGN neuron (ON-centre *X*-) and its retinal input by the simultaneous recording of the pre-synaptic potentials (B) and the post-synaptic spikes (C) from the neuron. Stimulus was 0.06 deg in width, frequency 2.5 Hz, luminance 30 cd/m². Background, 0.2 cd/m². The ordinates in (B) and (C) were normalized by taking the mean values of responses to 32 different stimulus lengths as 1.0 (1.0 = 110 spikes/sec for ganglion cell, 27.6 spikes/sec for LGN cell). The oblique lines are linear regression of responses over the DIR. The slope of the lines indicates the strengths of disinhibition. The difference of the slopes between the two curves is not significant ($P > 0.05$, *t*-test).

(Li & He, 1987) and for optic trace fibres (Li et al., 1991). The length– and/or area–response curves of the two stages of neurons showed an initial increase due to area summation in the receptive field centre, then a strong decrease caused by the antagonistic surround inhibition and at still larger or longer stimuli a secondary rise. A typical example for the retinal ganglion cells (ON-centre *X*-) is shown in Fig. 1A. With the stimulus centred at the RF centre and systematically enlarged, discharge rates were proportional to the size of the stimulus, as long as the stimulus was smaller than the RF centre (0.26 deg dia.), indicating an excitatory spatial summation within the centre. Larger stimuli caused suppression from the inhibitory surround and led to a response attenuation and a sharp fall in the curve. With further enlargement of the stimulus above 3.5 deg diameter (12 deg² area), the response amplitude recovered. Since direct stimulation of the area beyond the inhibitory surround alone with an annulus of appropriate dimensions never caused excitation at the light intensities used in our experiments, it suggests a disinhibitory region (DIR) outside the inhibitory surround. Disinhibition was seen with stimulus intensities between 3 and 30 cd/m² and extended up to 15 deg diameter and beyond for most of the cells recorded. As can be seen from Fig. 1A, the curve levelled off at 14–17 deg diameter (200–290 deg²) but may continue to rise at least slightly even for the largest stimuli used (360 deg²). For optic tract fibres, only for 5 out of 41, did the length–response curves show a plateau between 6 and 12 deg. DIR was found in 88% of the retinal ganglion cells, and for all eccentricities.

We were able to record the pre-synaptic potentials and the post-synaptic spikes simultaneously from three single LGN cells. The length–response curves, based on the pre-synaptic activity (*S*-potentials) of the input optic fibre, and on the post-synaptic spikes of the lateral geniculate cell were compared. Figure 1B and C shows an example from such recordings. The two curves always had similar shape, indicating identical dimensions for the centre, surround and outer-surround (disinhibitory) areas for the corresponding retinal and the geniculate neurons. The slopes of the secondary rising phase of the two curves also show that the strengths of the disinhibitory mechanisms, at the two levels, were not significantly different ($P > 0.05$, *t*-test). This suggested to us that the disinhibition region is determined mainly by the extensive neuronal network within the retina.

Transfer images by visual neurons

To demonstrate the role of the disinhibitory region in image information transmission, we recorded single cell activity from the lateral geniculate nucleus of cat and performed spatial "convolution" of the real receptive fields with a test image in a way as detailed below. This

procedure allows to demonstrate the pattern of spatial distribution of neuronal responses to the image across a two dimensional array of cells from the one recorded. A photograph of a table-tennis ball and its shadow comprised the visual stimulus (test image) (Fig. 2A). The illuminated surface of the ball provided an evenly-varying brightness gradient, and the shadow, an extended dark area. There were also borders with different contrast in the picture. Figure 2B is a quantitative expression of the relative luminance distribution over the ball surface and the shadow through one horizontal line as indicated by the arrow in Fig. 2A. The picture (20 by 20 deg in size) was projected onto the tangent screen. The luminance of the brightest zone (the upper-right of the ball) was 30 cd/m^2 and the darkest zone (the shadow), 2.2 cd/m^2. The picture was scanned, under computer control, in such a way that each part of the picture traversed, systematically, the RF of the cell (Creutzfeldt & Nothdurft, 1978). Different scan directions, usually horizontal and vertical, to and fro, were used. Scan movement was slow enough (2.6–5.2 deg/sec) to avoid temporal effects. Spikes were accumulated into a 50 by 50 bin raster, each bin representing the neuron's response when a particular part of the picture moved across the RF. Responses from different movement directions were then superimposed and normalized. The number of spikes in each bin was plotted as a two-dimensional display to demonstrate the response pattern (transfer image) of the individual neurons (Fig. 3A–C), in which density is proportional to spike frequency, the brightest region representing the cell's maximum spike count. With a diaphragm of variable diameter in front of the screen, stimulation could be restricted to the centre (c), or to centre plus surround ($c + s$). With whole field scanning (without the diaphragm), the areas stimulated involved both the classical centre/surround regions and the extensive disinhibitory outer-surround ($c + s + os$). By comparing the transfer pictures produced by the whole field scanning to those with diaphragm-restricted scanning, the role of the disinhibitory outer surround area in image information processing and transmission was evaluated.

Figure 3 is a typical example from an ON-centre X-cell. Figure 3A is the response picture of the cell when only the centre area of the RF was exposed to the scanned stimulus with a 0.6 deg diameter diaphragm. The cell behaved as a photo-detector and the areal brightness of the image was transmitted correspondingly. With a larger diaphragm (4 deg dia.), both the excitatory centre and the inhibitory surround were stimulated (Fig. 3B), the mean activity became much weaker. This can be seen by comparing the total counts of spikes in response to the $c + s$ stimulation (2788 spikes) with that to pure c-stimulation (9973 spikes) (see the numerals at the upper-right corners in Fig. 3A and B). Furthermore, the response profile to $c + s$ stimulation reproduced, principally, the borders of the ball and shadow; the brightness gradients over the ball surface and the uniform dark area within the shadow, however, disappeared and looked similar to the background. When the extensive area beyond the classical receptive field was also exposed to the stimulus scan, the total sum of spikes increased again (9216 spikes), and the brightness differences of the ball and the dark area of the shadow re-emerged. In addition, the borders of the image still remained enhanced. Interestingly, a neurophysiological representation of Mach bands, i.e. the dark bands along the borders of shadow and of the ball, can be clearly seen only in the $c + s + os$ condition. Since the resolution of the transfer images was limited by the small number of rasters (50 by 50 bins) and the discharge level in each bin was subjected to spontaneous variation from time to time, quantitative comparisons of the brightness distribution of the transfer images of the cell with that of the test image (shown in Fig. 2B) is difficult.

Transfer images of OFF-centre cells showed similar processing as for ON-centre cells. Figure 4 is an example. The transfer image for the central 0.5 deg area of the receptive field (Fig. 4A) appears like a negative of the original photograph (compare to Fig. 2A). The dark area of the original picture (shadow and the background) caused high-frequency discharges and vice versa. With a 5.5 deg $c + s$ exposure, border enhancement occurred and prominent bright and dark bands were seen (Fig. 4B). However, the areal contrast disappeared. As for the ON-centre cells, areal contrast partly recovered and border enhancement remained when the extensive area outside the classical RF was also exposed (Fig. 4C). By contrast with ON-centre cells, that the total count of discharges of the image showed less variation under different exposure conditions, may be due to the excitatory nature of the antagonistic surround.

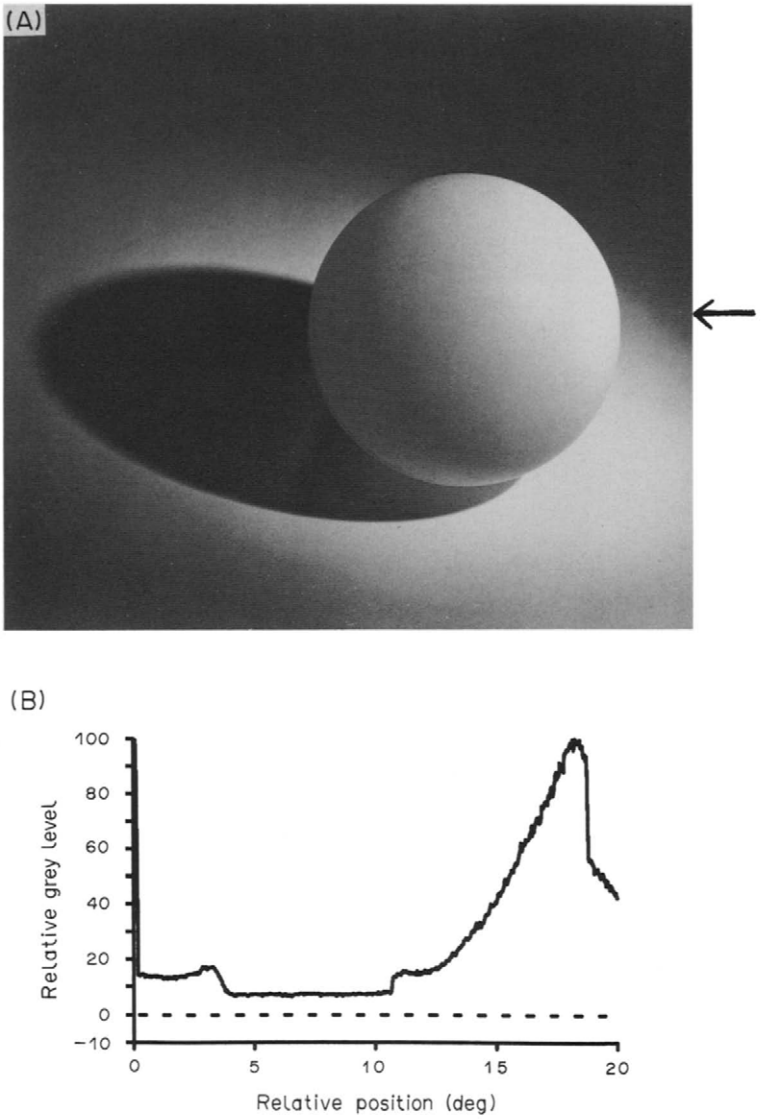

Fig. 2. (A) A photograph of a table-tennis ball used for demonstrating the transfer image of single lateral geniculate neurons and the mathematic model. The picture has a smoothly varying luminance gradient and an extended dark shadow. The luminance of the brightest zone of the ball surface was 30 cd/m^2 and the darkest zone (the shadow), 2.2 cd/m^2. It was 20 by 20 deg in size after being projected onto a tangent screen. (B) The quantitative expression of the spatial distribution of luminance through one horizontal scanning as indicated by the arrow in (A).

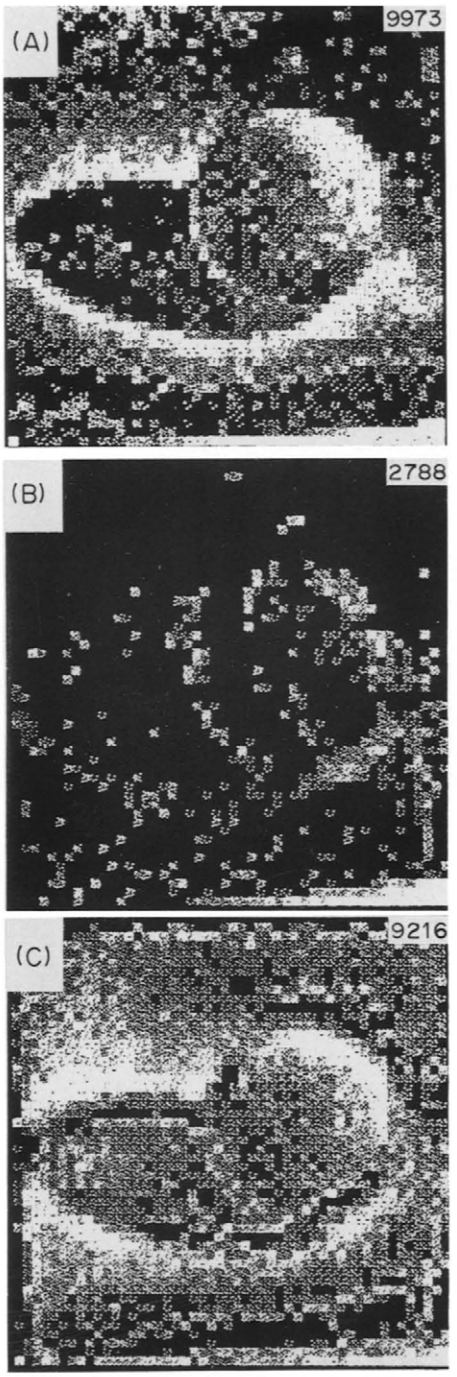

Fig. 3. Two-dimensional response profiles (transfer images) of a lateral geniculate neuron (ON-centre *X*-) showing the contribution of different RF mechanisms to image information transmission. The stimulus pattern is shown in Fig. 2A. The picture was scanned so that each part of it traversed, systematically, the RF of the cell. Scan speed 2.6 deg/s, 50 by 50 bin raster. The number of spikes in each bin is represented by the density of dots (the brightest area representing the maximum spike count). In total, 64 density levels are represented. (A) shows the transfer image of the cell when the RF, except for the central 0.6 deg, was covered by a mask; (B) when a 4 deg area including both centre and surround of the RF was open; (C) when the whole field, i.e. the centre and the surround plus DIR, was exposed. The numerals at the upper-right of each picture indicate the total number of spikes in the whole transfer image.

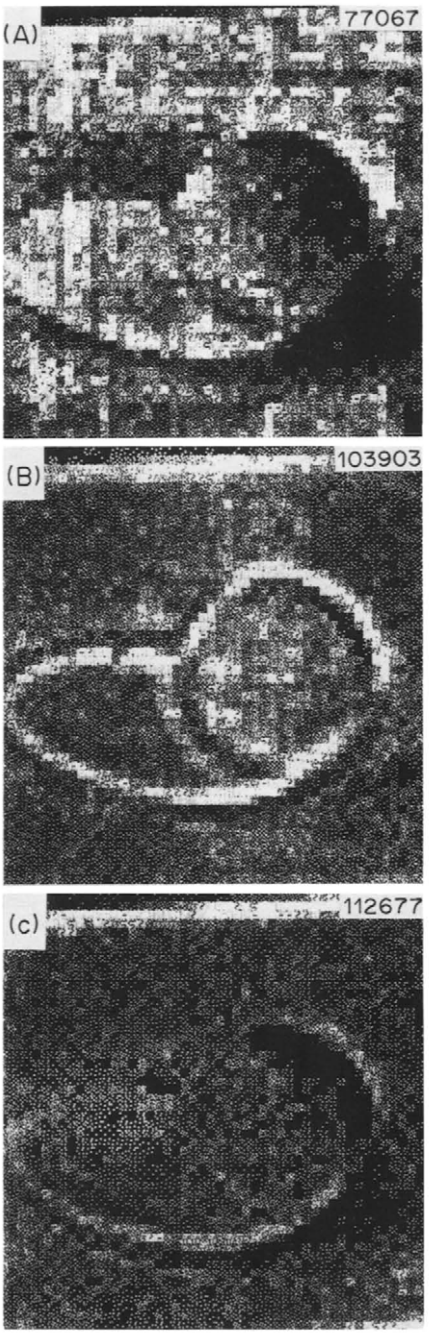

Fig. 4. Transfer images of an OFF-centre *X*-LGN cell. The stimulus and experimental procedure were the same as that described in Fig. 3A–C. (A) the transfer image of the cell when only the central 0.5 deg area was exposed to the stimulus; (B) when a 5.5 deg area $(c + s)$ was free; (C) when the whole field $(c + s + os)$ was exposed.

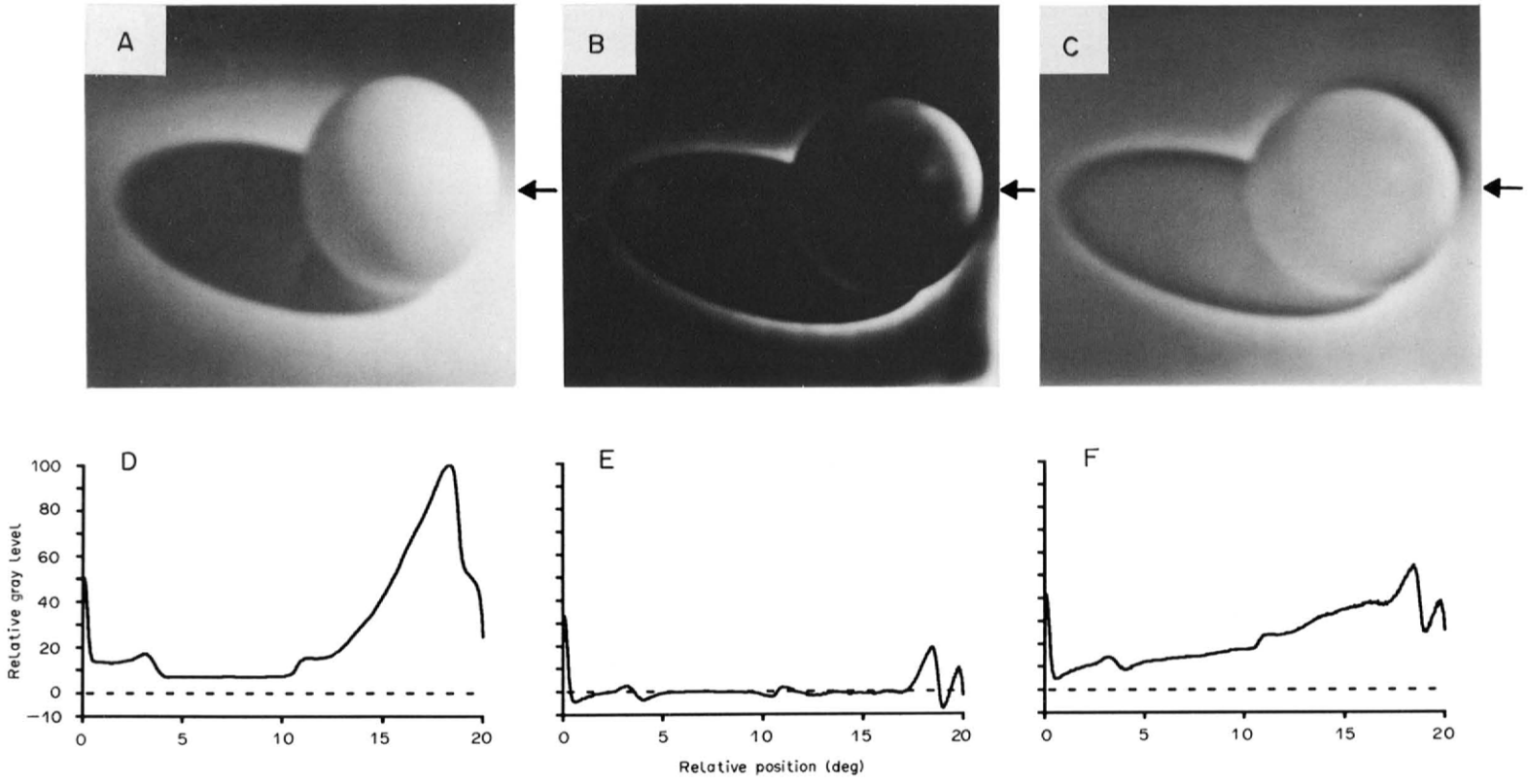

Fig. 5. Transfer images of the three-gaussian model of the receptive field. (A–C). The role of DIR in brightness information transmission of an image was demonstrated by processing the same picture with the mathematic model based on equations (1) and (2). The same photograph (shown in Fig. 2A) was scanned by a digital TV scan system with 512 by 432 pixels and 256 grey levels. The transfer images of the model were displayed on a high-resolution monitor after being processed by different components of the model. The model parameters used are; $A_1 = 100$, $A_2 = 4$, $A_3 = 0.08$; $\sigma_1 = 0.2$, $\sigma_2 = 1$, $\sigma_3 = 5$. (A) shows the calculated transfer image when only the centre mechanisms was involved; (B) the area included both the centre and surround of the RF; (C) when all three areas (centre, surround and DIR) were included. The curves in (D–F) are quantitative expressions of the grey levels of (A–C), respectively, through one horizontal scanning as indicated by the arrows in (A–C).

Mathematic model based on three Gaussian functions

We produced the quantitative analysis of the length- and/or area-response curves by fitting the data with a modified "Difference of Gaussians" model based on the algebraic sum of three Gaussian functions representing respectively the centre, surround and the outer-surround mechanisms of the receptive field. The difference of Gaussians model (Rodieck, 1965) postulates that the ganglion cell's response is equal to the difference between the signals from the centre and the surround. Sensitivity is assumed to be a Gaussian function of distance from the receptive field middle in both mechanisms. However, since the Gaussian representing the centre mechanism is narrower and shows a higher peak than that representing the surround, the centre mechanism dominates the surround mechanism at the middle of the receptive field and the surround signal is the major determinant at outer locations. The modified model employed in this report differs from the original model by adding a third positive Gaussian representing the outer surround disinhibitory mechanism with an extremely low sensitivity and wide space extent.

$$I(x,y) = A_1 \exp\left[\frac{-(x^2+y^2)}{\sigma_1^2}\right] - \left\{A_2 \exp\left[\frac{-(x^2+y^2)}{\sigma_2^2}\right] - A_3 \exp\left[\frac{-(x^2+y^2)}{\sigma_3^2}\right]\right\}. \quad (1)$$

$I(x,y)$ is the sensitivity profile of the receptive field. A_1, A_2 and A_3 represent the peak sensitivity values for the centre, surround and outer-surround mechanisms (discharges/deg^2), respectively. σ_1, σ_2 and σ_3 are the radii of the centre, surround and outer-surround mechanisms at which the sensitivity of each mechanisms has reached $1/e$ of the peak sensitivity value. The equation assumes that the sensitivity profiles of the three mechanisms are distributed as Gaussians, that they are circularly concentric with their peaks overlapped at the middle of the receptive field centre, and that they summate linearly from all parts of the receptive field. By choosing appropriate parameters of the model, good fit could be obtained to nearly all data from which the disinhibitory region was shown, even though the model assumes circular symmetry and the stimulus was square. A typical example is illustrated in Fig. 1A. The line through the data points is calculated by:

$$R = \iint_S L(x,y)\, I(x,y)\, dx\, dy \quad (2)$$

where $L(x,y)$ is relative stimulus intensity over space S, S represents stimulus area. The goodness of fit of the model to the area-response function of the cell allows the derivation of separate radius and sensitivity parameters for the three regions (see Table 1). In Table 1, A was normalized by taking the centre sensitivity as 100. $A\pi\sigma^2$ represents the integrated effect of each individual mechanism over the entire area.* As one might expect, the comparable values of the products $A_1\pi\sigma_1^2$ (=5.31) and $A_2\pi\sigma_2^2$ (=4.89) show that the effectiveness of the centre and surround mechanisms were nearly equal and therefore their effects on cell activity cancelled each other when both areas were completely illuminated. On the other hand, the multiple $A_3\pi\sigma_3^2$ (=2.26), which represent the effectiveness of the extensive area outside the classical surround, might provide up to 50% compensation for the neuronal activity to overcome the antagonistic surround cancellation and thus help the transmission of the brightness levels over an extended area. This compensation may reach a complete level, if only the transient component of responses was concerned in the effect (Li et al., 1991). Since this mechanism has an extremely weak sensitivity ($A_3 = 0.02\%$ of A_1) and depends mainly on spatial summation over a wide area ($\sigma_3 = 46\sigma_1$), it would not counteract the border enhancement caused by the local interaction of the centre/surround mechanisms.

Table 1. The RF parameters derived from the mathematic model

RF area	A	σ (deg)	$A\pi\sigma^2$
Centre (1)	100.00	0.13	5.31
Surround (2)	1.08	1.20	4.89
DIR (3)	0.02	6.00	2.26

Transfer images by the three-Gaussian model

The role of the disinhibitory outer surround in brightness information transmission was also illustrated by transforming the image using the mathematic model based on equations (1) and

*$A\pi\sigma^2 = \int_{-\infty}^{+\infty}\int_{-\infty}^{+\infty} A \exp[-(x^2+y^2)/\sigma^2]\, dx\, dy$.

(2), which closely approximates the responsiveness and transfer function of LGN cells. For this purpose, the same stimulating photograph was scanned by a computer-controlled digital TV scan system (Datacopy series 900). Mathematically, the picture is defined by a function $f(x, y)$ (coordinates in the image plane correspond to spatial locations), which are the grey levels at a regularly spaced array of points. We used an array of 512 by 432 pixels and the brightness at each pixel were measured in terms of 256 grey levels (8 bit). All values outside the picture were assumed to be zero. This digital picture was then displayed on a high-resolution monitor (Graphic controller AYDIN 5218) before (Fig. 2A), or after, processing by the model (Fig. 5A–C). The model parameters used are approximately those listed in Table 1 which best match the responses of the cell shown in Fig. 1A. Figure 5A represents the calculated transfer image when only the centre mechanism $\{\text{term } A_1 \exp[-(x^2+y^2)/\sigma_1^2]\}$ was involved. The output grey level at a given point depends on the local input grey level and sensitivity weighting of the centre mechanism (A_1). The picture appears similar to the original but was apparently blurred at the borders (compare Fig. 5A to Fig. 2A) depending on the size of the centre ($\pi\sigma_1^2$). Figure 5B shows the contribution of the inhibitory surround mechanism $\{\text{term } -A_2 \exp[-(x^2+y^2)/\sigma_2^2]\}$ to image processing. The output level, at a point, is determined by the difference of the inputs from the same point, i.e. the centre area, and from its neighbourhood, the surround

$$\{A_1 \exp[-(x^2+y^2)/\sigma_1^2] - A_2 \exp[-(x^2+y^2)/\sigma_2^2]\}.$$

The whole picture became much darker and the grey levels of the extended areas of the image disappeared due to the cancellation of the inhibitory mechanism. By contrast, the edges of the ball and shadow became prominent. Note that, as in Fig. 3B, the enhancement was only seen on the bright side of the edges in this case. As soon as a disinhibitory mechanism $\{A_3 \exp[-(x^2+y^2)/\sigma_3^2]\}$ was added (Fig. 5C), the average output grey level increased again, and the transfer property of the low spatial frequency components was clearly improved. As was shown in the single unit recordings (Fig. 3C), the smooth transitions in brightness of the ball, and the uniform dark area of the shadow reappeared, although not completely. The borders of the image remained enhanced and, only in this case, were both the bright and dark bands seen on each side of the edges. The transfer functions with different combinations of the receptive field components are shown in Fig. 5D–F. The curves are the response profiles along one horizontal scanning path as indicated in Fig. 5A–C (arrows). The curve in Fig. 5D, which represents the quantitative expression of transfer function of the centre area alone, appears to be a replication of Fig. 2B, but with blur at the edges and smoothening of the high frequency noise over the ball surface. Figure 5E shows the effect of the antagonist inhibitory surround, which leads to a complete loss of the brightness information of the shadow and the ball (compare Fig. 5E to Fig. 2B). The wavelets above and below zero level (dotted line) show the bright and dark components of Mach bands along the contrast borders. The existence of the dark band, however, is only hypothetical, since the mean activity level is actually zero and there is no possibility for the cell to differentiate between a negative and a zero response. The dark bands could clearly be seen only when the outer surround was involved and the mean activity was raised again by the disinhibitory mechanisms (compare Fig. 5F to E and C to B). In this case, the bright bands remained as prominent as is shown in Fig. 5E. The maximum brightness of the transfer image, however, was reduced to about one half of its original (compare Fig. 5F to D), as could be predicted from the area–response function.

DISCUSSION

Extent of the disinhibitory area

On the basis of quasi-intracellular recordings in cat lateral geniculate nucleus, Singer and Creutzfeldt (1970) suggested a model whereby an ON-centre geniculate cell receives field-centre input from an ON-centre retinal fibre, and surround input from several OFF-centre fibres. This model was supported by the observations of Hammond (1971–1973) and Maffei and Fiorentini (1972). The model predicts that an ON-centre geniculate neuron RF will possess an excitatory annular zone (outer surround) beyond the inhibitory surround, formed from the antagonistic surrounds of retinal fibre inputs whose centres constitute the inhibitory surround. Maffei and Fiorentini (1972) suggest that the fibre input to the geniculate surround is of the same type as that to field centre (via an

inhibitory interneuron). In either case, the implications of convergence are basically the same. Hammond (1972, 1973) made extracellular recordings from single optic tract fibres and cells in layers A and A_1 of LGN in cat and presented suprathreshold annuli with different outer-and inner diameters and identical quantum flux per unit area concentrically over the receptive field centre of an isolated unit. They found that geniculate cells possessed a weak disinhibitory surround beyond the inhibitory surround, but the same stimuli produced no disinhibition in retinal fibres. At the same time, Ikeda and Wright (1972a, b) demonstrated that "disinhibition" is not a property solely in the LGN, but that it occurred already for the retinal ganglion cells. They used intermittent spots either lighter or darker than the background, or two such spots, one at the centre of the receptive field and the other at varying distances from the receptive field centre. They found that the disinhibitory surround is strong and narrow in "sustained" cells but weak and laterally spread in "transient" cells. The extent of the outer surround was about 3–5 deg for transient cells and 1 deg or less for sustained cells, deduced from the figures in their reports.

By analyzing length– and/or area–response functions of retinal ganglion cells and lateral geniculate neurons (Li & He, 1987; Li et al., 1991), the disinhibitory area we have observed is much larger than that reported by the former investigators (Hammond, 1972, 1973; Maffei & Fiorentini, 1972; Ikeda & Wright, 1972a, b). One obvious explanation of this difference is that, as has been pointed out by Ikeda and Wright (1972a, b), the appearance of the disinhibitory area are closely dependent on stimulus size and intensity. As it has been mentioned in the results, the strength of disinhibition is very low compared to the excitatory and inhibitory processes (of the order of 0.02% of the centre sensitivity). When the field is tested by small spot or annulus stimuli, only the most central part of the outer surround might show a weak effect on cell responses. By taking advantage of spatial summation over increasing area, however, all the three mechanisms are able to be maximally activated (in sequence). This provided a suitable way for showing the spatial interactions between the three zones. For each cell examined, the stimulus, which coincides in size with the centre of its RF, excited the centre mechanism maximally and the maximum suppression of the centre response was produced with stimulus area which covered simultaneously the whole centre and surround. Only in this case, i.e. on the basis of the strongest suppression of the centre activity, the disinhibitory effect caused by further increasing stimulus areas could be revealed more prominently as a reduction of the surround inhibition and a recovery of the centre excitability. The boundary of disinhibitory area was revealed by the start of the plateau of the secondary rise in area– or length–response curves. The disinhibition region thus determined possess an extent up to 15 deg on an average, even for sustained cells.

On the basis of the extensiveness of the area and the "silent" nature (there is no response to direct stimuli) of the effect, it is appropriate to distinguish the DIR from the centre-surround-convergence determined disinhibitory surround. The functional role of the DIR is based on those characteristics.

Role of the disinhibitory area

To describe the different features of visual contrast, two types of spatial contrast were distinguished (Békésy, 1968): (a) *Mach-type contrast* appears as an over-shoot and under-shoot of luminance on the lighter and darker sides of boundaries, being of the order of only a few minutes of arc in human vision; (b) *Hering-type contrast* covers a much larger area and produces gradients in brightness sensation. The classical centre/surround antagonism is generally assumed to be the neuronal basis of Mach-type contrast. The neuronal mechanisms for Hering-type contrast, which is related to homogeneous perception of brightness, however, have not yet been adequately studied. One difficulty is that there appears to exist a contradiction between the two types of visual contrast. As for most cells centre and surround mechanisms are more or less balanced, combined stimulation results in a cancellation effect and, as a consequence, a reduction in responsiveness to low-spatial frequency components may occur. On the other hand, a compensation for the centre/surround antagonism may reduce the border enhancement. In both cases, the image quality will be downgraded.

The generality of existence of the extensive DIR in the afferent visual pathway may suggest a triple concentric organization of receptive field with two opposite antagonisms, i.e. centre-excitation vs surround-inhibition and surround-inhibition vs outer-surround-disinhibition. A three-Gaussian model which takes into account

the three mechanisms, as well as the two opposite antagonisms is put forward in the present work. The model matches parametrically to the actual response of the cell (Fig. 1A) and reproduces the transfer images of the visual neuron considerably well when convoluted with it (compare Fig. 3A–C to Fig. 5A–C). The quantitative demonstrations suggest that the disinhibitory mechanism may compensate the low frequency loss by increasing the general level of neuronal activation. At the same time, i.e. when the disinhibitory region raised the neuronal activity into its linear range, as was shown in Fig. 3C and Fig. 5C and F, both the bright and dark components of Mach Bands were revealed, and different grey levels of the visual image were represented around a mean level of activation of the neurons. Since the sensitivity of the disinhibitory mechanism is extremely low and its influence on neuronal activity depends mainly on spatial summation over a wide area, this compensation would not impair the border enhancement caused by the local centre/surround mechanism. Yet, the maximum brightness response is reduced if the whole picture is presented through an open aperture as compared to the small aperture exposure (compare the peak level in Fig. 5F to that in D). This corresponds to the phenomenon of darkness induction of the Hering-type brightness contrast (Creutzfeldt, Lang-Malecki & Wortman, 1987).

Acknowledgements—This research was supported by the Science Fund of the Chinese Academy of Sciences, the National Natural Science Foundation of China and by Max-Planck-Institute for Biophysical Chemistry, Göttingen, F.R.G. to C.Y.Li. We thank Professor O. D. Creutzfeldt, Dr H. C. Nothdurft, Dr D. A. Tigwell and Dr J. Yin for helpful comments on the manuscript, Dr H. C. Nothdurft for providing software, and Mrs X. C. Hsu for technical assistance.

REFERENCES

Baumgartner, G., Brown, J. L. & Schulz, A. (1965). Responses of single units of the cat visual system to rectangular stimulus patterns. *Journal of Neurophysiology, 38*, 1–18.

Békésy, G. von. (1968). Mach- and Hering-type lateral inhibition in vision. *Vision Research, 8*, 1483–1499.

Bishop, P. O., Kozak, W., Levick, W. R. & Vakkur, G. J. (1962). The determination of the projection of the visual field on the lateral geniculate nucleus in the cat. *Journal of Physiology, London, 163*, 503–539.

Cleland, B. G., Dubin, M. W. & Levick, W. R. (1971). Sustained and transient neurons in the cat's retina and lateral geniculate nucleus. *Journal of Physiology, London, 217*, 473–496.

Cleland, B. G., Levick, W. R. & Sanderson, K. J. (1973). Properties of sustained and transient ganglion cells in cat retina. *Journal of Physiology, London, 228*, 649–680.

Creutzfeldt, O. D. & Nothdurft, H. C. (1978). Representation of complex visual stimuli in brain. *Naturwissenschaften, 65*, 307–318.

Creutzfeldt, O., Lange-Malecki, B. & Wortman, K. (1987). Darkness induction, retinex and cooperative mechanisms in vision. *Experimental Brain Research, 67*, 270–283.

Enroth-Cugell, C. & Robson, J. G. (1966). The contrast sensitivity of retinal ganglion cells of the cat. *Journal of Physiology, London, 228*, 649–680.

Fischer, B. & Krüger, J. (1974). The shift effect in the cat's lateral geniculate neurones. *Experimental Brain Research, 21*, 225–227.

Hamasaki, D. I. & Sutija, V. G. (1979). Classification of cat retinal ganglion cells into *X*- and *Y*-cells with a contrast reversal stimulus. *Experimental Brain Research, 35*, 25–36.

Hammond, P. (1971). Chromatic sensitivity and spatial organization of cat visual cortical cells: Cone–rod interaction. *Journal of Physiology, London, 213*, 475–494.

Hammond, P. (1972). Spatial organization of receptive fields of LGN neurones. *Journal of Physiology, London, 222*, 53–54p.

Hammond, P. (1973). Contrast in spatial organization of receptive fields at geniculate and retinal levels: Centre surround and outer surround. *Journal of Physiology, London, 228*, 115–137.

Ikeda, H. & Wright, M. J. (1972a). Outer excitatory ("disinhibition") surround to receptive fields of retinal ganglion cells. *Journal of Physiology, London, 224*, 26–27p.

Ikeda, H. & Wright, M. M. (1972b). The outer disinhibitory surround of the retinal ganglion cell receptive field. *Journal of Physiology, London, 226*, 511–544.

Kuffler, S. W. (1953). Discharge patterns and functional organization of mammalian retina. *Journal of Neurophysiology, 16*, 37–68.

Li, C. Y. & He, Z. J. (1987). Effects of patterned backgrounds on responses of lateral geniculate neurons in cat. *Experimental Brain Research, 67*, 16–26.

Li, C. Y., Chang, Y. R., Chen, P. S., Hsu, H. C. & Wang, H. (1979). Role of sustained neurones of cat lateral geniculate nucleus in processing luminance information. *Scientia Sinica, 22(3)*, 359–371.

Li, C. Y., Zhow, Y. X. & Pei, X. (1991). Extensive disinhibitory region beyond the classical receptive field of cat retinal ganglion cells. Submitted.

Maffei, L. & Fiorentini, A. (1972). Retinogeniculate convergence and analysis of contrast. *Journal of Neurophysiology, 35*, 65–72.

McIlwain, J. T. (1964). Receptive fields of optic tract axons and lateral geniculate cells: Peripheral extent and barbiturate sensitivity. *Journal of Neurophysiology, 27*, 1154–1173.

Ramachandran, V. S. (1988). Perceiving shape from shading. *Scientific American 259(2)*, 58–65.

Rodieck, R. W. (1965). Quantitative analysis of cat retinal ganglion cell response to visual stimuli. *Vision Research, 5*, 538–601.

Rodieck, R. W. & Stone, J. (1965). Response of cat retinal ganglion cells to moving visual patterns. *Journal of Neurophysiology, 28*, 819–832.

Singer, W. & Creutzfeldt, O. D. (1970). Reciprocal lateral inhibition of on- and off-centre neurones in lateral geniculate body of cat. *Experimental Brain Research, 10*, 311–330.